Plasma Processing System Based on Electron Beam Ionization

D. Leonhardt, M.M. Balkey, R.F. Fernsler, R.A. Meger, and D.P. Murphy,
Naval Research Laboratory, Plasma Physics Division, Washington, DC; and S.G. Walton
and D.D. Blackwell, SFA, Inc., Largo, MD

Key Words: Plasma species, Electron density, Ion sources, Etching/cleaning

ABSTRACT

Electron beam (e-beam) ionization is both efficient at producing plasma and scalable to large area (square meters) with beam energy and density. With the plasma production emanating from the electron beam, the plasma is largely decoupled from the surrounding vacuum system. Chamber and substrate geometry are no longer constraining factors, permitting not only proportional scalability but immense freedom in chamber design and construction materials. Thus, e-beam produced plasmas provide better control of plasma constituents over larger areas with higher efficiencies than conventional discharge sources.

In our laboratory, modulated (0.01^{-10} millisecond pulse length, up to 50% duty cycles) and continuous e-beam produced plasmas are being studied with the goal of using their unique characteristics to modify the surface properties of materials. Planar plasma distributions are generated by injecting a magnetically collimated sheet of 2-5 kV, 1^{-10} mA/cm^2 electrons into neutral gases (O_2, N_2, Ar, SF_6 and their mixtures). From *in situ* diagnostic techniques, spatially and temporally resolved plasma characteristics are presented along with plasma-to-surface ion fluxes (via mass spectrometry). The demonstrated attributes of these plasma sources over conventional plasma sources are extremely low electron and ion energies, localization of ionization source away from chamber walls and system scalability.

INTRODUCTION

The use of plasmas for dry processing of materials has become vital in numerous fabrication industries [1,2]. Dry processing is preferred in many applications because generally it provides a wider spectrum and higher densities of reactive species, better control of those species, more directionality of ion fluxes, and less contamination and waste. Moreover, processes like etching, deposition and surface activation of materials can be carried out *in vacuo*, that is, in a somewhat clean vacuum environment and as part of a multi-step fabrication process. Many different types of plasma sources have been used in such endeavors, although the basic discharge physics remains the same; an applied electric field heats electrons until they have acquired enough energy to ionize the background gas, which is typically well above 10 eV. This description pertains to high density ($\geq 10^{11}$ cm^{-3}) inductively coupled (ICP), helicon, electron-cyclotron resonance (ECR) discharges, low density (10^8 - 10^{10} cm^{-3}) capacitively coupled, dc glow, rf diode discharges, and hybrid (magnetically enhanced) discharges.

A major drawback of these conventional plasma sources is the lack of control over the plasma. In the majority of these devices, after initiation the plasma electrons rapidly (< 1 microsecond) thermalize, with their resultant energy distribution given by the Boltzmann equation. The applied electric field continues to heat the electrons which sustain the plasma, traveling rapidly through the background gas, ionizing and exciting it. Because of the high ionization energies of most gases, only the high energy 'tail' of the plasma electron energy distribution actually supplies the electrons capable of ionization. The plasma sustenance relies on the balance between this ionization and all the loss mechanisms, which depend on the plasma density, plasma gas, and source geometry. Typically, plasma electron temperatures (T_e) range from 2 to 8 eV (where 1 eV = 11,600 Kelvin) while the positive ions remain around room temperature (0.03 eV).

Looking more closely at the electrons in these conventional plasma sources, the solid black curves in Figure 1 show two electron energy distributions (with T_e = 1 and 5 eV) while the dashed curves are cross sections for ionization and excitation of argon. It can be seen from Figure 1 that ionization varies strongly with T_e, since only a small portion of the plasma electrons (shaded area) are capable of ionizing the background gas. In almost all cases, T_e must rise to an appreciable fraction of the gas ionization energy (W_i) in order to produce sufficient ionization. Consequently, T_e is determined by plasma loss mechanisms in conventional sources. The balance of these competing mechanisms is difficult to predict and is usually set by stable operating conditions.

© **2002 Society of Vacuum Coaters** 505/856-7188

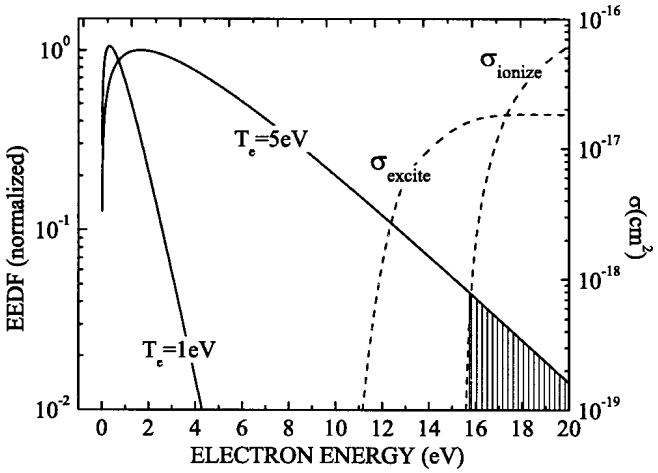

Figure 1: Electron energy distribution functions (solid) and excitation/ionization cross sections (dashed) for argon.

From Figure 1 we see that a large fraction of plasma electrons are energetic enough to excite the gas, through *inelastic* collisions where the electron energy gets stored in an excited state of the atom. In the noble gases, the lowest excited states are roughly 3/4 the ionization potential. In molecular gases (or mixtures containing molecular gases) there are many more inelastic collision channels due to additional electronic levels and the increased degrees of freedom (e.g. vibration) of the molecular states. Figure 2 illustrates the case of nitrogen.

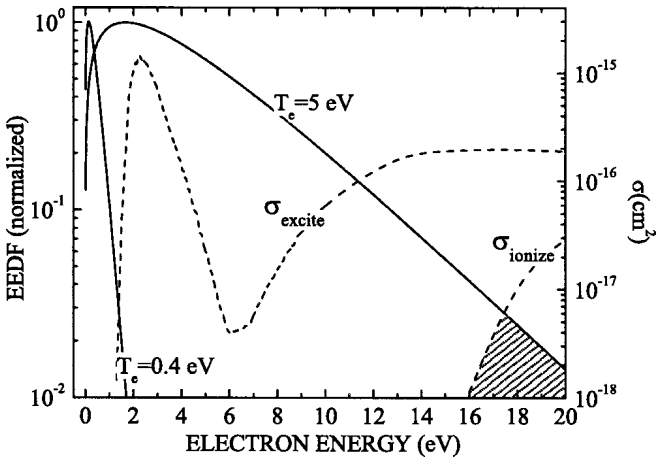

Figure 2: Electron energy distribution functions (solid) and excitation/ionization cross sections (dashed) for nitrogen.

As seen in Figure 2, the dominant inelastic process at low electron energies is molecular excitation, such that little of the energy absorbed goes into ionization. These non-ionizing inelastic collisions ultimately serve to heat the gas, since additional collisions typically lead to redistribution of molecular vibrational states and not ionization. The increased population of vibrational levels thus heats the neutral gas, which in turn heats the plasma ions since the ions are created out of the neutral species. Again, only the high energy 'tail' of the electron energy distribution is energetic enough to ionize the molecule directly. In many cases, two-step processes (including Penning ionization) can also contribute significantly to gas ionization.

The present article discusses a less common plasma source which uses an electron beam to directly ionize the gas, thereby decoupling the plasma electrons from the primary ionization process. When a high energy (>> W_i) electron beam passes through a gas, the dominant energy loss process is ionization of the gas, followed by dissociation and excitation. Hence, an electron beam can efficiently ionize a gas while putting little energy into inelastic collisions. The plasma electrons, which are not strictly part of the ionization process now, have a severely diminished role since the ionization source driving the plasma is the e-beam and not the high energy 'tail' of the plasma electrons. Moreover, plasma electrons are rapidly cooled by the background gas, through virtually all collision processes available. The resultant plasma electron temperatures are thus extremely low, 1-2 eV in atomic gases and < 0.5 eV in molecular gases. Because of the additional ionization from cooling the plasma electrons, the plasma density is typically 2-4 orders of magnitude larger than the beam density. The relative scaling of these electron distributions are shown in Figure 3, along with the nitrogen cross sections from Figure 2.

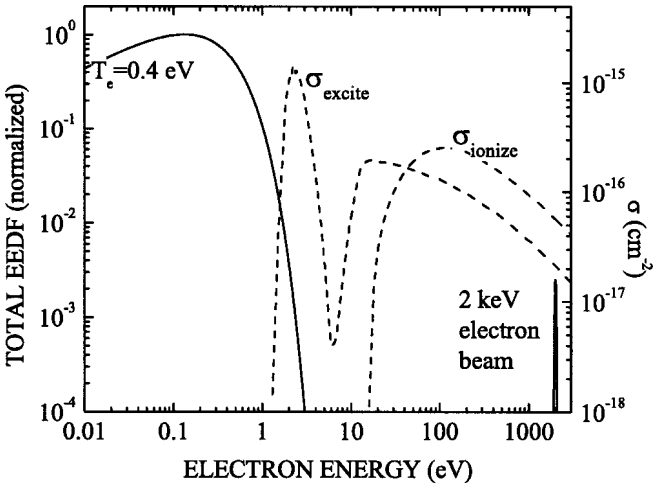

Figure 3: Inelastic collision cross sections (dashed) and illustrative electron energy distribution function (solid) for an electron-beam produced plasma in nitrogen.

With the ionization process being driven by an e-beam instead of by externally heating the plasma electrons (through rf or dc fields), plasma operating conditions become much broader. The beam ionization is not confined by any geometric configuration and the plasma characteristics are controlled independently by the beam current and energy. Furthermore,

energy distributions of ionized species are determined by the gas composition instead of by the species with the lowest ionization threshold. E-beam produced plasmas have been used to fill large areas or volumes with reactive species while maintaining a high level of efficiency over a wide parameter regime.

EXPERIMENTAL APPARATUS/TECHNIQUES

Plasma Sources and Chambers

Identical or nearly identical e-beam produced plasmas were created in a variety of vacuum systems constructed from plexiglass, (38 cm in diameter x 50 cm tall; base pressure 0.05-4 mtorr), aluminum (50 cm in diameter x 65 cm tall; base pressure ~ $5x10^{-7}$ torr) and stainless steel (50x120x50 cm; base pressure < $5x10^{-8}$ torr). Details of particular vacuum systems will be given with the appropriate diagnostic (see below). Electron beams were generated by a hollow cathode which has been discussed at length in the scientific literature [3]. The cathode consisted of a 1 cm wide channel, approximately 1.5 cm deep and 22 cm long, in 2.5 cm diameter brass rod stock. An insulating sheet (teflon or machinable ceramic) and ground shield cover the inactive cathode surfaces to suppress unwanted electrical breakdowns. The electron beam generated by the cathode is physically skimmed by a stainless steel shim stock anode containing a 1 x 20 cm slot aligned with the cathode hollow and placed ~ 5 cm downstream. A second solid anode, placed ~ 25 cm past the first slot acts as the beam dump. The beam between the anodes is centered in a pair of 50 cm diameter Helmholtz coils, which provides an axial magnetic field of ~165 Gauss with uniformity better than 2% between the anodes. The resultant e-beam sheet was therefore defined by the slotted anode (1 cm x 20 cm) and the distance (~25 cm) to the beam dump anode. The cathode was driven with high voltage (2.5 kV) pulses, 0.5-5 ms in length at repetition rates of 1-50 Hz. A continuous cathode source has also been used in our laboratory by floating a hollow cathode discharge operating at low voltage (~ 300 V) and accelerating plasma electrons through a high voltage grid.

Gases were introduced into the systems either through mass flow controller units (MKS 1179 Series) or variable leak valves (Leybold). Chamber pressures were then set by throttling the vacuum (turbomolecular) pump with various gate or butterfly valves. The purity of gases used in these experiments was 99.999% argon and >99.8% nitrogen and oxygen. Convectron® and/or Pirani-type vacuum gauges were used to determine operating pressures and the reported readings have been corrected for the particular gas type.

Langmuir Probes

Langmuir probe measurements were carried out in the plexiglass and aluminum vacuum chambers. Due to higher operating pressures, various gas compositions and usually low duty factors, surface contamination of Langmuir probes made it necessary to continuously heat the probe externally to achieve consistent data. Typical probe construction consisted of a 0.25 mm (10 mil) thoriated tungsten wire protruding 2 mm out of an 0.156 cm diameter, four bore alumina tube. A 4 cm 'hairpin' of nichrome wire was fed through two bores and was used to heat the probe tip locally. Ceramic paste coated the exposed portion of the heater element. For all but the last two inches of the probe, all wires and connections were enclosed in a grounded tube which was shielded from the plasma with another alumina tube. It was found that if the probe temperature was kept at around 500°C, reproducible results could be obtained. Typical probe I-V traces were obtained by applying a bias voltage to the probe and monitoring the collection current through the probe by measuring the voltage across a standard carbon resistor. Data were recorded on a digital oscilloscope or using boxcar averagers (Stanford Research Systems SR250) with 1-10 μs sample gates positioned during and after the e-beam.

In the plexiglass chamber, microwave transmission measurements were carried out to calibrate electron densities measured with the Langmuir probe. A pair of 20 dB horns straddled the plasma sheet outside the chamber, and a Hewlett-Packard frequency synthesizer (1-25 GHz) was used as the microwave signal source. The microwave signal is amplitude modulated at ~20 kHz to clearly identify baseline levels of the signal during the plasma modulation. These calibrations gave high confidence in repeatability when similar probes were put into other systems.

Since contaminated probes have dramatic effects on the determination of the plasma potential and electron temperatures [4], emissive probes were used to independently corroborate the plasma potentials determined in the externally-heated Langmuir probe measurements [5]. Similar ceramic and tungsten materials were used for this probe as well. Emission of the probe was controlled by a [floating] DC power supply operated in constant current mode. Complete sets of emission characteristics were not possible in the presence of the magnetic field used to collimate the e-beam; auxiliary plasmas along the magnetic field lines were easily ignited by the e-beam plasma and sustained when the beam went off, even at low probe emission currents.

Mass/Ion Energy Analyzer

Mass spectrometry was carried out in the aluminum and stainless steel vacuum chambers using a quadrupole mass analyzer (Hiden EQP300). The mass spectrometer was differentially pumped and sampled plasma species through a small orifice in the 5.7 cm diameter head before energy and subsequent mass separation. No noticeable deviation in the data was seen when the orifice size was changed from 100 to 50 microns, implying little if any perturbation of the plasma due to the presence of the orifice. The orifice was grounded and positioned parallel to the e-beam, simulating a substrate surface for materials' processing applications. In the mea-

surements here, the stage was located 1 cm away from the edge of the e-beam [6]. Detection of charged species was averaged over large times (comparable to the e-beam pulse width) for global information on individual specie distributions. For high temporal resolution, ions were counted as single-particles using a gated pulse counter. Further details are available in Reference [6].

Processing Stage

A sample processing stage designed similar to the head on the EQP was used to expose standard negative photoresist samples to plasma sheets under varying conditions. The front plate was stainless steel which was electrically isolated with a boron nitride spacer from the surrounding ground support. A thermocouple was embedded in the insulator to monitor the front plate temperature. Applying radio frequency (rf) signals at 13.56 MHz allowed appreciable induced dc bias levels to form on the stage from the e-beam plasma before parasitic rf breakdown occurred. Photoresist was spun onto silicon substrates and patterned in-house with a ~ 50 nm chromium mask to interrogate material removal rates and process anisotropy. Test samples (1 cm^2) were cleaved from parent wafers containing patterned photoresist and mounted with silver print adhesive.

RESULTS AND ANALYSIS

Langmuir Probes

Langmuir probe measurements in these plasmas have been extremely reproducible across vacuum platforms, once the surface contamination issues were addressed appropriately. Typical plasma parameters measured for a 90 mtorr argon plasma showed electron densities (n_e) and temperatures (T_e) to be 2-4x10^{11} cm^{-3} and 1.2-1.4 eV in the ionization region, respectively, and plasma potentials (V_{pl}) of 5-7 V. Two centimeters outside the ionization region, T_e and n_e drop to approximately one half these values, as does V_{pl}. In molecular gases, plasma temperatures are significantly lower. For nitrogen and oxygen plasmas at 50 mtorr, T_e = 0.2-0.3 eV, respectively, and n_e ~ 2-2.5x10^{11} cm^{-3} while V_{pl} = 1-2 V. Inelastic collisions in these gases cause the T_e to drop much lower while still maintaining high electron densities. Even trace amounts of molecular gases added to noble gases will have similar electron characteristics. However, addition of strongly electronegative gases which allow low energy plasma electrons to attach, like sulfur hexaflouride, rapidly consume the low energy plasma electrons and form negative ions, leaving only hotter plasma electrons which have low probability of attachment. In these plasmas when the electron density drops to < 0.1% the negative ion density, the plasma potential drops to ~ 0 V as positive and negative ion currents become comparable.

Once the e-beam is turned off, the source of ionization disappears and the plasma decays or is said to be in an 'afterglow'. In atomic gases, it is believed that the plasma decay is diffusion dominated, since recombination of atomic ions is a three-body and therefore unlikely process. In molecular gases, it is believed that the plasma decay is dominated by electron-ion recombination. In this case, after the beam ceases, the plasma density decays from its density at the end of the pulse, n(0), according to $dn_e/dt = -\beta n_e^2$, where β is the recombination coefficient and electrons are the only negative charge carriers. Solving this equation, we see that the ion density varies as $n(t) = n(0)/[1+\beta n(0)t]$ where t is the time after the pulse. As a verification of this decay mechanism, the temporal profile from probe measurements is shown in Figure 4 for a plasma created by an 800 μs e-beam pulse.

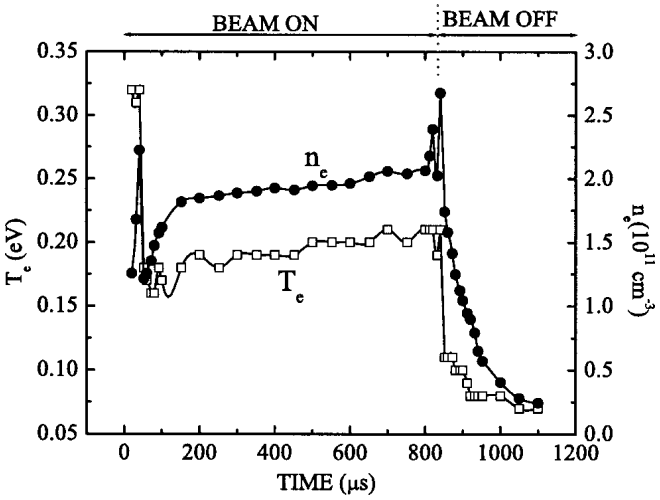

Figure 4: Temporal Langmuir probe measurements for an electron-beam produced nitrogen plasma.

An experimental recombination coefficient was calculated by fitting $1/n_e$ from the afterglow portion in Figure 4 to a straight line. This fit yields $\beta = 8.1x10^{-8}$ cm^3/s for the initial decay. In N_2 the recombination coefficient varies as [7] $\beta = 4.3x10^{-8}x[T_e]^{-0.39}$ which when equated to our experimental value, results in an afterglow plasma temperature of 0.19 eV, in excellent agreement with the data in Figure 4. Because the plasma temperature decreases with time, a perfect fit would not be expected over the entire decay range. While this result is somewhat fortuitous, given the weak temperature dependence of the recombination coefficient, the low electron temperatures (<< 1 eV) measured nevertheless support the plasma decay mechanism. A similar analysis in the O_2 discharge (using [8] $\beta = 2.4x10^{-8}x[T_e]^{-0.5}$) results in the same afterglow temperature, which is slightly higher than the measured 0.15 eV temperature derived from probe measurements.

Mass/Ion Energy Analyzer

In atomic gases, dominant ion species at the stage are the parent atom followed by ~ 5% of the doubly ionized atom. In molecular gases (O_2 or N_2), the atomic ion is dominant with ~ 10% being the molecular ion. This is presumably due to

dissociative ionization directly from the electron beam, although the probability of this ionization mechanism does not account for such disproportionate ratios. When gases are mixed, ion species are commensurate with the relative gas density, as shown in Figure 5 where relative ion species are given as the background gas is changed from pure argon to pure nitrogen. Secondary ions are also shown on the same scale with similarly filled/open symbols as the dominant ion. It can be easily seen that dominant ion increases monotonically with gas concentration. Such control over ion flux is contrary to conventional discharges where the dominant ion species is determined by the lowest ionization threshold and not gas mixture.

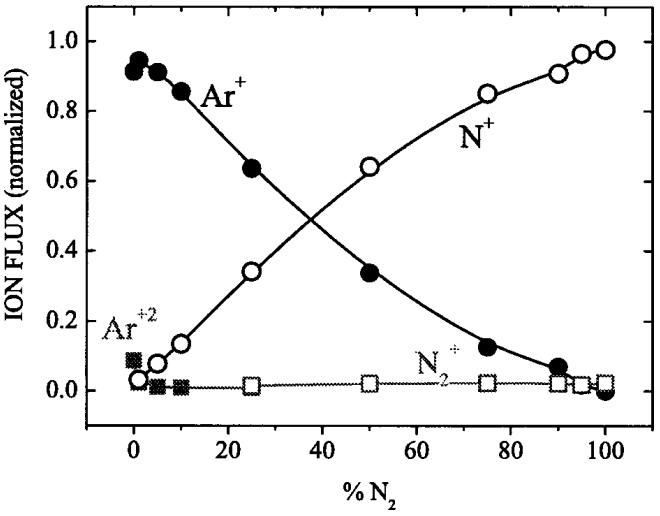

Figure 5: Ion fluxes measured for an electron-beam produced plasma as feedstock gas is changed from argon to nitrogen.

The energy of the incident ions measured was also quite different from conventional discharges. With the energy passband of the EQP fixed at discrete values and single-ion counting over very small time intervals, the data in Figure 6 were acquired for a one millisecond e-beam pulse. Upon ignition of the plasma, a large flux of high energy (3 eV) ions is seen, then rapidly decreases. A similar spike is seen in electron temperature and density (cf. Figure 4). The signal for lower energy ions (1 eV) build up (or reach the analyzer) later during the pulse, becoming the largest fraction. These ion energies are commensurate with the measured plasma potentials (~1 V) as expected – the ions can only get energies as large as the plasma's internal fields. (In conventional sources, plasma potentials are typically an order of magnitude larger and therefore ions hit surfaces with significantly more energy.) After the pulse, the atomic ions rapidly charge exchange with background gas to form molecular ions. All of the molecular ions in turn recombine with plasma electrons as seen previously in the Langmuir probe results.

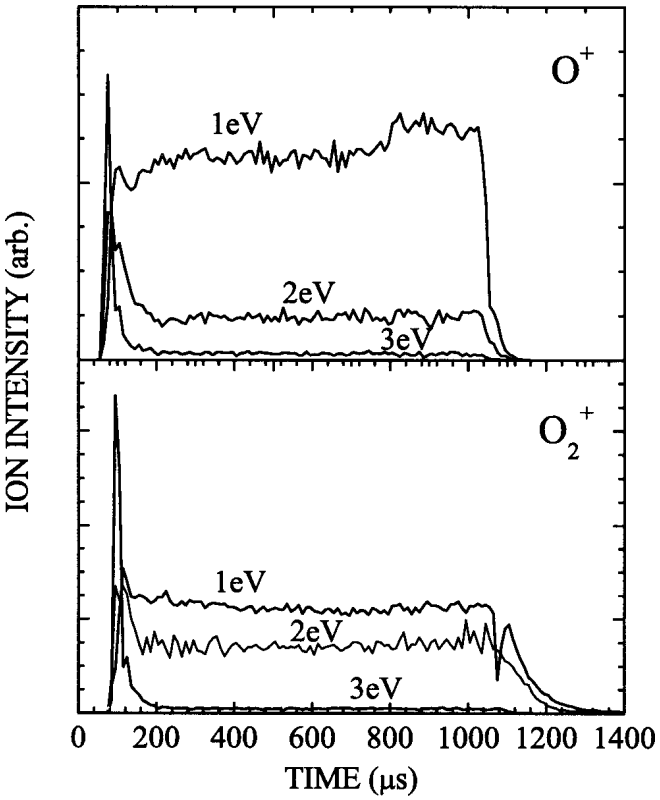

Figure 6: Temporally and energy-resolved ion fluxes measured in an electron-beam produced oxygen plasma.

Processing Tests on Photoresist Material

In order to further investigate these plasma characteristics and try to control them effectively, surface modification tests were carried out in the aluminum vacuum chamber with a 55 mtorr oxygen plasma. Because of the very low ion energies, no material removal was seen at room temperature with a grounded substrate. By applying an rf bias to the stage, the additional energy imparted to the ions appeared to stimulate the desorption of volatile species, whose removal rate increased nearly linearly as the stage bias was increased to –100 V. Poor pattern transfer (or anisotropy) was seen at low ion energies but became quite good above –75 V.

Typically hydrocarbon film removal with oxygen plasmas in conventional plasma sources is carried out without additional substrate biasing, but plasma potentials are also much larger (10-20 V) and rapidly heat the surface of the sample as well, both of which may stimulate surface activation. In order to determine whether surface reactions were neutral (O, O_3) flux limited, the oxygen was removed from the gas mixture and replaced with argon while the substrate bias was kept at –50 V (and 10% duty factor). The results are shown in Figure 7. It is seen that the oxygen partial pressure drops to below 20% before an appreciable drop in removal rate is noticed. Thus,

surface coverage is complete above 20% O_2 partial pressure and it does not appear that the ion species are as important as ion energy.

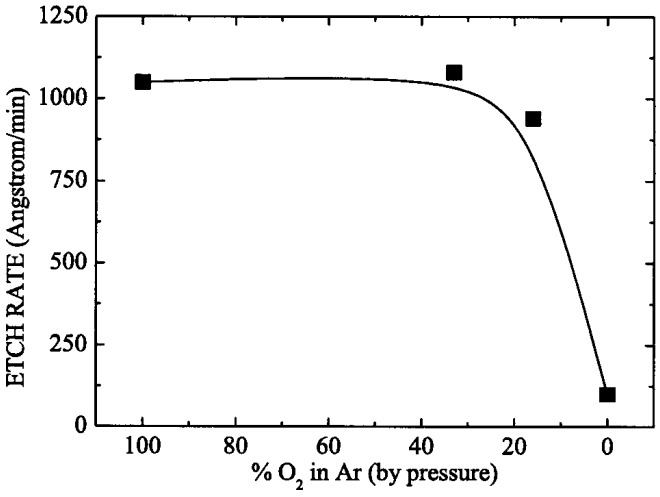

Figure 7: Photoresist etch rate as oxygen partial pressure is reduced. All samples have –50 V rf bias and were run at a 10% duty cycle.

SUMMARY AND CONCLUSION

In this work we have given a general overview of electron-beam produced plasmas and fielded a series of standard *in situ* diagnostics to augment the current level of understanding of these plasmas. Unlike conventional plasma discharges, these plasma electrons are not initiating ionization and therefore cool rapidly in the presence of background gas. Through temporally and spatially resolved measurements of electron and ion characteristics, we see localized high density ($> 10^{11}$ cm^{-3}) plasmas which have low electron temperatures (< 1.5 eV) and low internal fields which result in low ion energies as well. Very low electron temperatures < 0.5 eV (and therefore internal fields) are seen when molecular gases (e.g. O_2, N_2, SF_6) are present because of the additional cooling of plasma electrons by molecular vibrational levels. Also, because gas ionization is initiated by an electron beam, ion compositions can be predetermined by gas fractions and their energies controlled through external fields.

These general characteristics were applied to a simple chemical system of standard photoresist polymer in an oxygen-rich plasma environment. Room temperature removal of polymer showed a linear dependence on ion energy and indicated that reactive species were not flux limited. Anisotropic pattern transfer was seen with ion energies ≥ 75 V. Such dependencies are typically not seen in conventional plasma sources where the sheath voltage drop is much larger. These aspects make electron beam sources interesting prospects for materials modification especially where low energies and control of thermal properties are important process parameters.

ACKNOWLEDGMENTS

This work is supported by the Office of Naval Research. M.M.B. gratefully acknowledges support from the National Research Council. The authors would also like to thank Mr. A.K. Noll and R. Lanham for their technical support in the laboratory.

REFERENCES

1. J.B. Fenn Jr., W.C. Kittler Jr., D. Lievens, R. Ludwig, G. Phillips and A. Taylor, "Roll-to-Roll Sputter Web Coater: A Status Report," Vacuum Technology and Coatings, 2 (3), 56-65 (2001); M. F. Nichols, "Plasma Polymerized Thin Films for Corrosion Control on Electronic Devices," Vacuum Technology and Coatings, 2 (5), 56-61 (2001); A. Grill, Cold Plasmas in Materials Fabrication, (IEEE Press, New Jersey, 1994).

2. D.M. Mattox, "Plasma Technology: Plasma Chemistry, Etching and Deposition," Society of Vacuum Coaters Educational Guides to Vacuum Coating Processing, (SVC Publications, New Mexico, 1995).

3. D. Leonhardt, S.G. Walton, D.D. Blackwell, W.E. Amatucci, D.P. Murphy, R.F. Fernsler and R. A. Meger, J. Vac. Sci. Technol. A, 19, 1367 (2001); R.F. Fernsler, W.M. Manheimer, R.A. Meger, J. Mathew, D.P. Murphy, R.E. Pechacek and J.A. Gregor, Physics of Plasmas, 5, 2137 (1998).

4. W.E. Amatucci, P.W. Schuck, D.N. Walker, P.M. Kintner, S. Powell, B. Holback and D. Leonhardt, Rev. Sci. Instrum., 72, 2052 (2001).

5. N. Hershkowitz, "How Langmuir Probes Work," Plasma Diagnostics: Dischrage Parameters and Chemistry, O. Auciello and D.L. Flamm eds., (Academic Press, Inc., San Diego, 1989), p. 146.

6. S.G. Walton, D. Leonhardt, R.F. Fernsler and R.A. Meger, 45th Annual Technical Conference Proceedings of the Society of Vacuum Coaters, 2002, Figure 1.

7. F.J. Mehr and M.A. Biondi, Phys. Rev., 181, 264 (1969).

8. P.M. Mul and J.W. McGowan, J. Phys. B: Atom. Molec. Phys., 12, 1591 (1979).